

The geology of the Gréixer area (La Cerdanya, Eastern Pyrenees): Sardinic, Variscan, and Alpine imprints

La geología del área de Gréixer (La Cerdanya, Pirineos orientales): huellas sárdicas, variscas y alpinas

ELOI GONZÁLEZ-ESVERTIT^{1*} , JÚLIA MOLINS-VIGATÀ² , ÀNGELS CANALS¹  y JOSEP MARIA CASAS² 

¹ *Departament de Mineralogia, Petrologia i Geologia Aplicada, Facultat de Ciències de la Terra, Universitat de Barcelona, C/ Martí i Franquès s/n, Barcelona, 08028, Spain.*

² *Departament de Dinàmica de la Terra i de l'Oceà, Facultat de Ciències de la Terra, Universitat de Barcelona, C/ Martí i Franquès s/n, Barcelona, 08028, Spain.*

* *Corresponding author: e.gonzalez-esvertit@ub.edu*

Abstract: We present new data of the pre-Variscan, Variscan, and Alpine evolution of the pre-Silurian rocks from the Gréixer sector (La Cerdanya area, Eastern Pyrenees). Structural analysis and detailed mapping of Cambrian-Ordovician and Upper Ordovician low-grade metasediments suggest the existence of three deformational events, together with the emplacement of an hectometric-sized quartz vein and the development of thrusts zones. We compare the results with other sectors close to the study area, and suggest that they form the southern (reverse) limb of a kilometre-sized E-W-trending south-verging “D₂” antiform of Variscan age. This fold was deformed by open NW-SE-trending south-verging “D₃” folds with gently north-dipping limbs of unknown age—Variscan or Alpine. Moreover, microstructural analysis and the structural attitude of the D₂ mesostructures suggest the existence of a pre-Upper Ordovician “D₁” deformational event that only affects the Cambrian-Ordovician metasediments. By comparison with neighbouring areas, an Alpine age for quartz vein emplacement and the development of thrust zones is suggested.

Keywords: structural analysis, giant quartz vein, Cambrian-Ordovician, Upper Ordovician, Eastern Pyrenees.

Resumen: Presentamos nuevos datos sobre la evolución pre-varisca, varisca y alpina de las rocas pre-Silúricas de los alrededores de Gréixer, en La Cerdanya, Pirineo oriental. El análisis estructural y cartografía de los meta-sedimentos de bajo grado metamórfico de edad cambro-ordovícica y ordovícica superior, sugieren la existencia de tres episodios de deformación así como el emplazamiento de cabalgamientos y de una vena de cuarzo de tamaño hectométrico. La comparación con otros sectores próximos sugiere que todos ellos forman el flanco sur (invertido) de un antiforme “D₂” kilométrico E-O con vergencia hacia el sur, de edad varisca. Este pliegue fue deformado por pliegues “D₃” posteriores, de orientación NO-SE y vergencia sur, cuyos flancos buzan moderadamente hacia el norte y cuya edad es desconocida, varisca o alpina. Además, el análisis microestructural y la disposición de las meso-estructuras D₂ sugieren la existencia de un evento de deformación “D₁”, anterior al Ordovícico Superior, que afectaría tan solo a la sucesión Cambro-Ordovícica. Por comparación con zonas vecinas, se sugiere una posible edad alpina para el emplazamiento de la vena de cuarzo y para el desarrollo de los cabalgamientos.

Palabras clave: análisis estructural; vena gigante de cuarzo; Cambro-Ordovícico; Ordovícico Superior; Pirineo Oriental.

1. Introduction

Pre-Silurian rocks cropping out in the basement of the Pyrenees record the imprint of pre-Variscan, Variscan, and Alpine deformation phases. The structural inheritance of these episodes is exceptionally well exposed throughout the La Cerdanya area (Eastern Pyrenees), where a low-grade metasedimentary succession crops out in, among others, the Gréixer,

La Molina and Talltendre sectors (i.e., Santanach, 1972a; Casas and Fernández, 2007; Casas, 2010; Puddu et al., 2019). These rocks have been deformed by various folding episodes and also host multi-sized quartz veins, from millimetric to centimetric thicknesses and metric lengths in the La Molina and Talltendre areas (Puddu et al., 2019; González-Esvertit et al., 2020) to metric thicknesses and hectometric lengths in the Gréixer area.

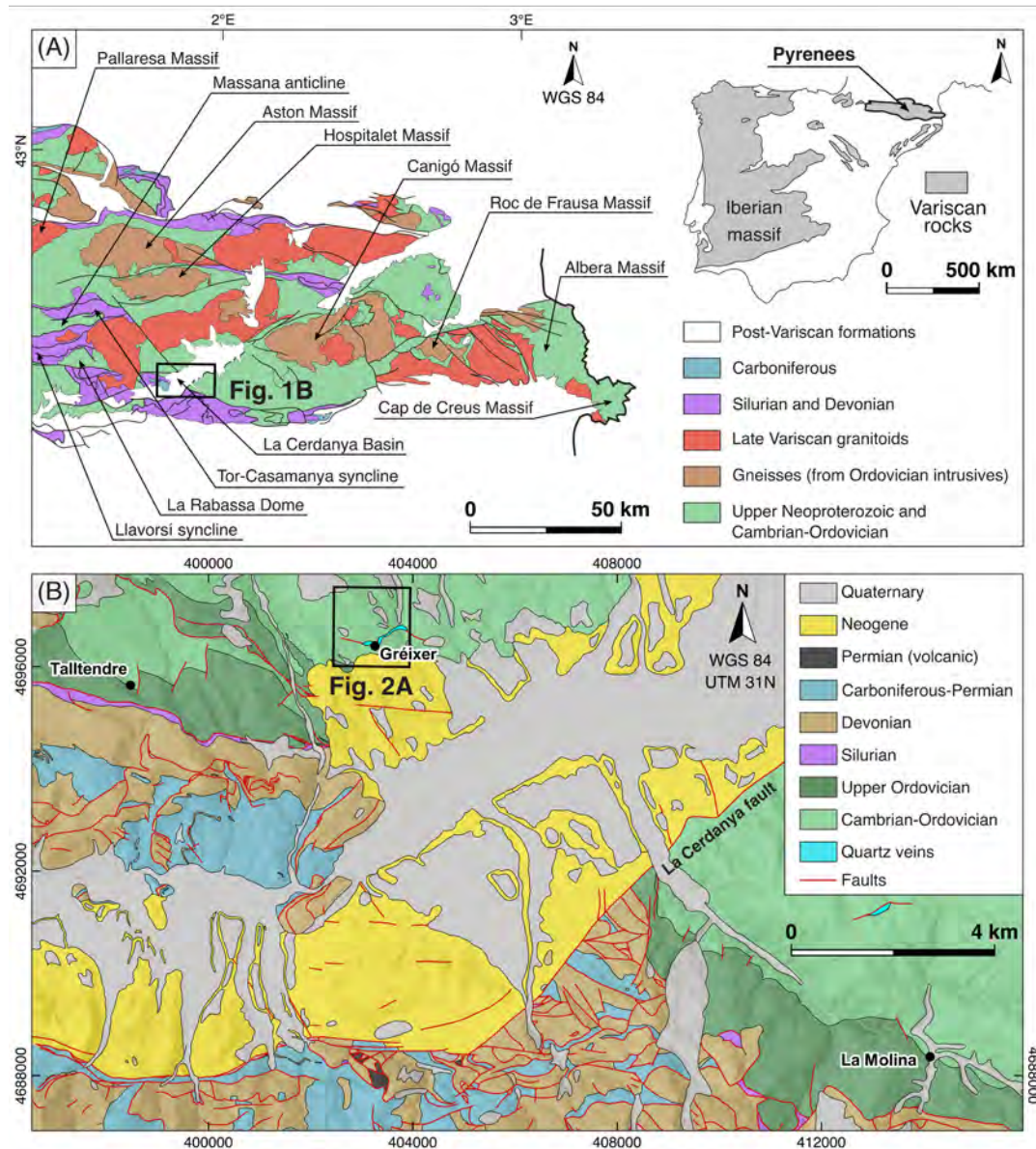


Figure 1. (A) Geological sketch map of the Eastern Pyrenees and its location on the Iberian Peninsula. (B) Detailed geological map of the La Cerdanya area, modified after Institut Cartogràfic i Geològic de Catalunya (1:25,000) and Instituto Geológico y Minero de España (1:50,000) (CC BY 4.0); note that the La Cerdanya normal fault separates the Gréixer and Talltendre sectors (in the hanging wall) from the La Molina sector (in the footwall).

Aiming to decipher the structural evolution of the pre-Silurian rocks of the La Cerdanya area, here we present a detailed geological map and structural analysis of the Gréixer sector, together with its structural comparison with the available data from neighbouring sectors. Furthermore, as the study of quartz veins helps to reconstruct the tectonic and thermal evolution of the rocks where they are hosted, we discuss the age and the structural controls on the emplacement of the hectometric-sized Gréixer vein.

2. Geological setting

The Pyrenees is an Alpine E-W trending fold-and-thrust belt formed from the Late Cretaceous to Miocene after the collision between Iberia and Eurasia (Roest and Srivastava, 1991; Muñoz, 1992; Rosenbaum et al., 2002). Along the central area of the orogen (i.e., the Axial Zone), the Alpine deformation exhumed a complete pre-Variscan basement succession, Late Neoproterozoic to Carboniferous in age, mainly made up of low- to medium-grade metasedimentary rocks (Fig. 1A). These rocks record Cadomian, Ordovician, and Variscan magmatism, and were affected by Sardic (Ordovician), Variscan, and Alpine deformational events, as well as by Variscan regional metamorphism (Santanach, 1972a, b; Muñoz, 1992; Casas, 2010; Navidad et al., 2018; Padel et al., 2018).

The study area is located near the town of Gréixer in the La Cerdanya area (Eastern Pyrenees; Fig. 1) and is made up of Cambrian-Ordovician and Upper Ordovician metasedimentary successions and Neogene sedimentary rocks (Fig. 2) (González-Esvertit et al., 2022a). Cambrian-Ordovician rocks from the Gréixer sector correspond to the uppermost part of the Jujols Group (Cavet, 1957; Laumonier, 1988) and are represented by the Serdinya Formation and its uppermost Font Frède Member (Padel et al., 2018). The Serdinya Fm. comprises a rhythmic alternation of millimetric to centimetric sandstone and shale layers. It was attributed to the Late Cambrian (Furongian)–Early Ordovician by Casas and Palacios (2012) on the basis of acritarch

remnants in the La Molina area, whereas a maximum depositional age of ca. 475 Ma was proposed by Margalef et al. (2016) according to the youngest detrital zircon population in the La Rabassa dome. In the Gréixer sector, the Serdinya Fm. contains two key centimetric levels: convoluted facies or soft-sediment deformation structures, interpreted to be formed during storm episodes or liquefaction processes, and quartzite layers. The quartzite levels become more recurrent upwards until reaching the Font Frède Member, which crops out scarcely in the study area and consists of a ca. 10 m-thick package of centimetric quartzite with decametric lateral extension (Fig. 2A). According to Padel et al. (2018), the Font Frède Member could represent the onset of an early Tremadocian regression. The overlying Upper Ordovician succession exhibits significant (100 – 1000 m) thickness variations and displays a fining upwards siliciclastic package with some carbonatic levels and volcanic intercalations. From base to top, Hartevelt (1970) defined five formations that can be identified along the pre-Variscan outcrops of the Pyrenees and the Catalan Coastal Ranges: the La Rabassa Conglomerate, Cava, Estana, Ansobell, and Bar Quartzite Fms. In the Gréixer sector, only the Cava Fm. has been identified. It is composed of feldspathic conglomerates and sandstones grading upward into variegated shales and fine-grained sandstones. This formation was attributed to the Katian (former Late Caradoc–Early Ashgill) by Gil-Peña et al. (2004) on the basis of abundant brachiopods, bryozoans, and echinoderms.

In the Pyrenees, the Upper Ordovician unconformity separates the Cambrian-Ordovician and the Upper Ordovician metasedimentary successions. This unconformity has been recognized near the study area in the La Molina and La Rabassa areas (Santanach, 1972b; Casas, 2010; González-Esvertit et al., 2020), the Tallendre sector (Casas and Fernández, 2007; Puddu et al., 2019), as well as in other Pyrenean massifs (Den Brok, 1989; García-Sansegundo and Alonso, 1989; Kriegsman et al., 1989; García-Sansegundo et al., 2004). It corresponds to the “Sardic” unconformity, also recognized in other domains of the NW Gondwana margin such as Sardinia, and their origin and significance are still

the subject of different interpretations (Cocco and Funedda, 2019). In the La Molina and Talltendre areas, Casas (2010), Casas et al. (2012) and Puddu et al. (2019) related the formation of this unconformity to pre-Upper Ordovician foliation-free open folds attributed to a Mid-Ordovician deformational event. This folding event was followed by a Mid-Late Ordovician extensional faulting coeval with the deposition of the lower part of the Upper Ordovician succession which, in some sectors, exhibits significant thickness variations (Casas, 2010).

As in the rest of the pre-Variscan rocks of the Pyrenees, a pervasive cleavage parallel to the axial surfaces of the main folds (S_2) is the most recognisable structure in both successions of the studied area. This S_2 cleavage can be correlated to the “ S_3 ” cleavage recognized in the Pallaresa, La Rabassa, and Orri domes and in the Tor-Casamanya and Llavorsí synclines (Fig. 1A) (Speksnijder, 1986; Poblet, 1991; Clariana and García-Sanseguno, 2009; Margalef and Casas, 2016) and has been classically linked to the main Variscan folding episode.

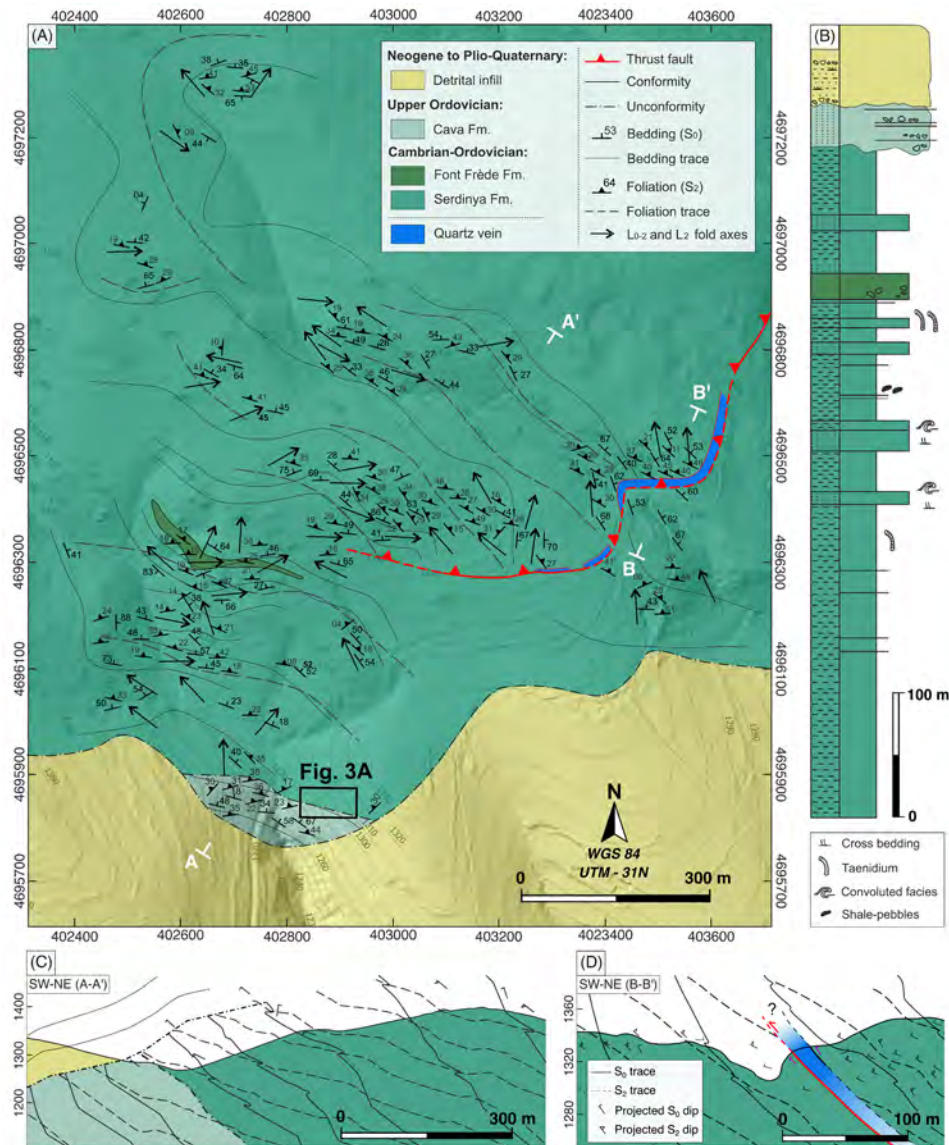


Figure 2. (A) Detailed geological map of the Gréixer area, (B) schematic stratigraphic log and (C, D) geological cross-sections. Location shown in figure 1B.

Alpine deformation involved the pre-Variscan successions from the La Cerdanya area within the Rialp-(Canigó) unit, the lowermost crustal thrust sheet of the Central-Eastern Pyrenees, which is overthrust by the Orri-(Cadí) and the Pedraforca-(Nogueres) units (Muñoz, 1992). These three units make up an antiformal stack with their basal thrusts dipping towards the north on the northern side of the chain, sub-horizontal in its central area and south-dipping at its southern contact with the Mesozoic-Cenozoic cover. According to Muñoz (1992) and the paleomagnetic data from McClelland & McCaig (1989) the main cleavage present in the pre-Variscan rocks of the Pyrenees was also displaced and folded during the antiformal stacking of these thrust sheets. Despite the southward displacement of ca. 150 – 160 km along these thrust sheets (Muñoz, 1992), Alpine metamorphism is absent and the internal deformation is moderated, so that the original characteristics of the Pyrenean basement rocks may be confidently reconstructed.

After the Alpine compression, Neogene extension in the Pyrenees gave rise to different intramontane basins. The La Cerdanya Basin (Fig. 1) was formed as a result of a half-graben development along the hanging wall of the La Cerdanya normal fault. Together with the La Seu d'Urgell, Rosselló, Conflent, and Capcir basins, the La Cerdanya Basin exhibits a Neogene to Plio-Quaternary infill of detrital (mainly lacustrine) deposits. In the La Cerdanya Basin these deposits directly overlap the pre-Silurian rocks in its northern area (Pous et al., 1986 and references therein), whereas the southern margin of the basin is bounded by the La Cerdanya normal fault, which separates the Gréixer and Talltendre sectors (in its hanging wall) from the La Molina sector (in its footwall) (Figs. 1, 2). According to the published cross-sections (Cirés et al., 1994) a minimum displacement of ca. 1000 m can be estimated for the La Cerdanya normal fault.

Within this framework, Cambrian-Ordovician and Upper Ordovician rocks from the La Molina and Talltendre sectors exhibit paleo-fluid circulation fingerprints represented by centimetric-width quartz veins (Puddu et al., 2019; González-Esver-

tit et al., 2020). Contrarily, in the Gréixer sector, a metric-width discontinuous quartz vein is present (Figs. 1B, 2A, 2D). An Alpine age and low fluid/rock ratio regimes have been recently proposed for the La Molina veins (González-Esvertit et al., 2020). However, the age and formation conditions of the Gréixer and other non-continuous km-scale veins that are spread throughout the Pyrenees are not yet well constrained (Ayora and Casas, 1983; Ayora et al., 1984; González-Esvertit et al., 2022b).

3. The Gréixer host rock structure

In the Gréixer area, the contact between the Cava and Serdinya Fms. (i.e., the Upper Ordovician unconformity) crops out scarcely due to the fact that it is almost entirely covered by Neogene rocks (Figs. 1B, 2A). Bedding planes in both successions exhibit a similar NW-SE trend with a reverse NE dip. However, close to the unconformity, the Cava Fm. beds dip less (ca. 31/354) than the Serdinya Fm. beds (ca. 58/019) (Figs. 3, 4A, 4B). At a regional scale, this contact can be considered as an angular unconformity (e.g., Casas and Fernández, 2007).

A poorly-developed slaty cleavage (S_1) defined by the orientation of phyllosilicate crystals can be identified at microscopic scale only within the Cambrian-Ordovician rocks of the Serdinya Fm. (Fig. 5B). The study area stands out for its well-developed cleavage (S_2) that exhibits a broadly uniform disposition (Figs. 3B, 3C, 5B), trending mainly NW-SE and dipping moderately to the NE (average value: 31/025) (Figs. 2A, 2C, 2D, 4C, 4D). At microscope scale, S_2 can be described as a crenulation cleavage affecting the previously developed S_1 surfaces (Fig. 5B). In the Cambrian-Ordovician and the Upper Ordovician rocks, S_2 cleavage is related to centimetre-sized D_2 folds, facing the NE and with “Z” asymmetry viewing down plunge (Fig. 3C). D_2 folds are well recognizable when affecting the bedding surfaces of the Cambrian-Ordovician rocks of the Serdinya Fm. due to its lithological and grain size variations. According to the bedding-cleavage relationship, minor S_0 fold asymmetry, and map scale fold geometry depicted by the bedding surfaces, the area

represents the southern (reverse) limb of a south-verging first-order hectometre to kilometre sized D_2 fold (Figs. 2, 3B, 3C). The quartzite of the Font Frède Member displays several well recognizable

examples of larger, decimetric-sized, D_2 folds (Fig. 3D). The larger size of the folds in the quartzite is probably due to its higher competence and layer thickness.

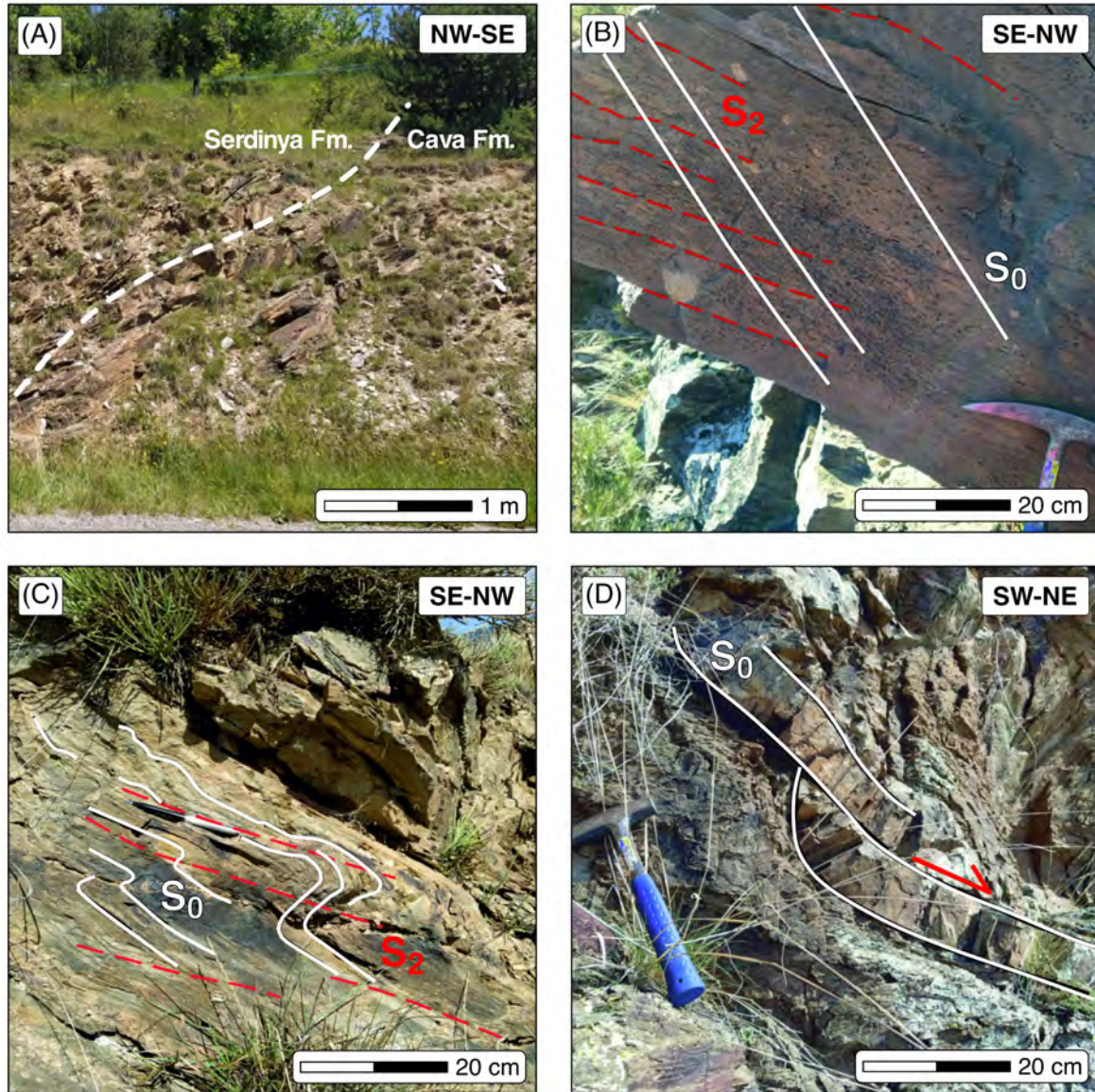


Figure 3. (A) The Upper Ordovician Unconformity splitting up the Serdinya and Cava Fms. (Location shown in Figure 2). (B) Relationships between the bedding (S_0) and cleavage (S_2) surfaces in the Cava Fm., which suggest that the study area belongs to a southern (reverse) limb of a south-verging first-order D_2 fold. (C) S_0 surfaces of the Serdinya Fm. exhibiting centimetre-sized D_2 folds with “Z” asymmetry, linked to the S_2 development. (D) Quartzite layers of the Font Frède Member showing a minor (decametric) SW-NE oriented thrust fault.

In the Cambrian-Ordovician rocks, bedding poles are mainly distributed along a NE-SW girdle with a maximum oriented ca. 39/033 (p axis 8/313) (Fig. 4A). It should be noted that poles to bedding are also dispersed along another girdle that is orthogonal to this one (Fig. 4A). The S_2/S_0 intersection lineation (L_{S_2/S_0}) and D_2 fold axis are dispersed and arranged on a girdle (31/020), which is coincident with the S_2 average value (Fig. 4C). Over this girdle, a NW-SE (05/298) maximum L_{S_2/S_0} value can be recognized, roughly coincident with the p axis deduced from the bedding disposition. The dispersion of the L_{S_2/S_0} and D_2 fold axes, together with the S_0 disposition (Figs. 4A, 4C), suggest the existence of a previous deformational event (D_1) that could be linked to

the development of the aforementioned S_1 cleavage (Fig. 5B), although no mesostructures related to this event have been identified at outcrop scale.

Despite cropping out in a reduced area—available data is therefore scarce (Figs. 4B, 4D)—the bedding surfaces of the Cava Fm. present a distribution on a single girdle (p axis 10/306) (Fig. 4B), suggesting that they are not affected by the D_1 deformational event, which in this case should be pre-Upper Ordovician in age. The fact that the L_{S_2/S_0} values in the Upper Ordovician rocks do not show a dispersion as marked as those from the Cambrian-Ordovician succession also suggests the existence of this pre-Upper Ordovician deformation event (Fig. 4C, 4D).

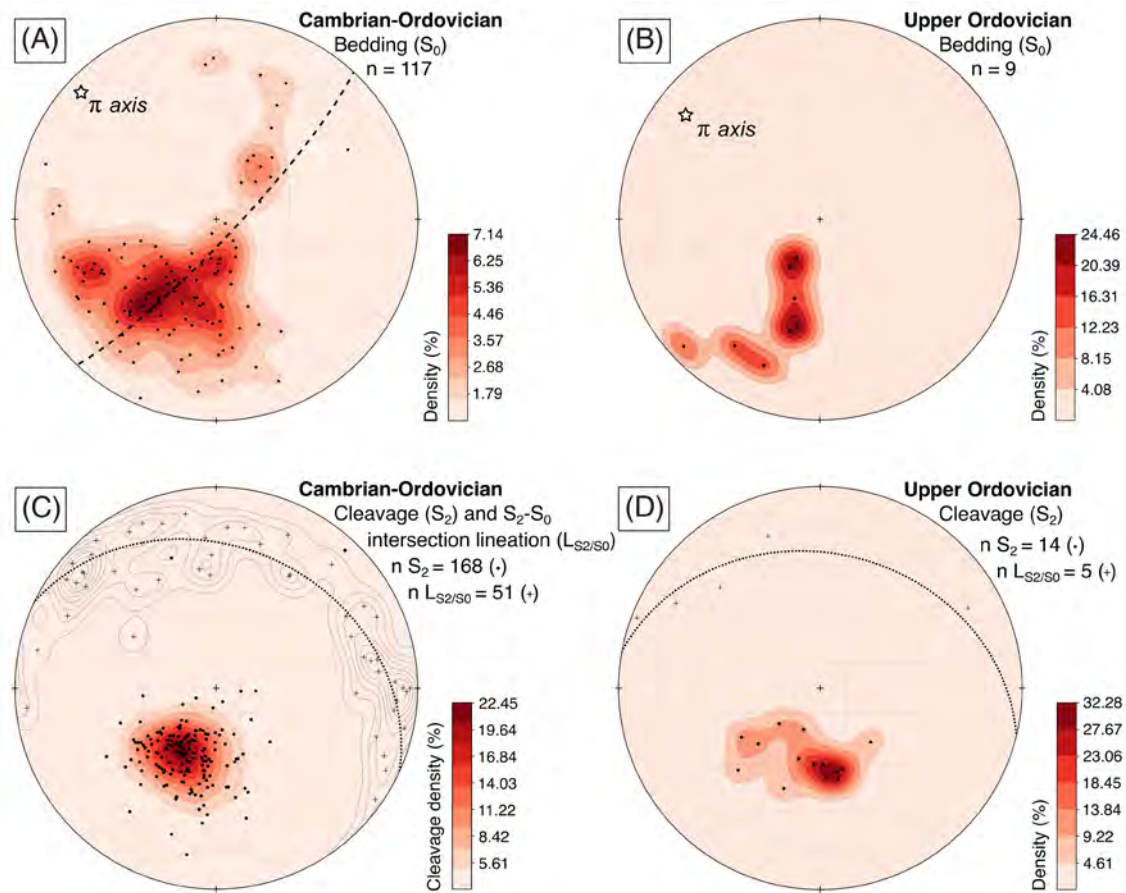


Figure 4. Equal-area lower-hemisphere stereoplots of the rocks from the Gréixer area: bedding surfaces of Cambrian-Ordovician (A) and the Upper Ordovician (B), cleavage and bedding-cleavage intersection lineation of the Cambrian-Ordovician (C), and cleavage of the Upper Ordovician (D). n is the number of measurements.

Brittle mesostructures can be found in the study area, including a metric-spaced joint set and a decametric-sized thrust fault zone (Figs. 2, 5C). NE-SW oriented joints are developed only in the host rocks surrounding the Gréixer vein. Joints dip moderate-to sub-vertically towards the SE or NW. Moreover, the boundaries of the Gréixer vein (see Section 4) exhibit the geometry of an E-W trending, south-directed thrust which postdates the D_2 folds and the S_2 cleavage (Figs. 2, 5C, 5D). This thrust is similar to others linked to quartz bodies located northwards of the study area (Cirés et al., 1994). The lithological uniformity of the Serdinya Fm. prevents one from quantifying the southwards displacement related to this thrust. A minimum post- D_2 moment of emplacement can thus be considered for this structure and, on the basis of their geometry and orientation, we propose an Alpine age.

4. The Gréixer quartz vein

The Gréixer vein (Fig. 5A) is located within Cambrian-Ordovician rocks and exhibits three NE-SW aligned hectometric-size quartz bodies (Fig. 2A), which share the same macrostructural features. Their core zones are broadly formed by massive milky quartz with scarce (5 – 15%) and partially silicified host rock fragments (Fig. 5E), 0.5 – 5 cm in size. The amount of these fragments increases notably (up to 80%) towards the limits of the quartz bodies (Fig. 5F), and thus in most cases it is not possible to recognize a net vein-Serdinya Fm. host rock border. Several stylolite-like dark surfaces are homogeneously distributed without preferential orientation along the massive quartz bodies, and the latter are also crosscut by more transparent micrometric to millimetric width anastomosing quartz veinlets (Fig. 5E). In some areas, vein limits are defined by 5 – 20 cm thick semi-continuous brecciated levels, where host rock fragments are embedded within a milky quartz mass (Fig. 5F). Moreover, main quartz bodies eventually narrow and branch into centimetric-width veins towards their terminations. These are the unique centimetric-width veins identified outside the main quartz bodies in the study area, thus indicating that silica precipitated in a spatially re-

stricted structure, more distinctively than at La Molina (González-Esvertit et al., 2020) or Tallendre (Puddu et al., 2019) sectors where numerous centimetric-width quartz veins are spread throughout.

Field evidence suggests that the Gréixer vein is spatially linked to the E-W trending south-verging thrusts identified in the study area (see Section 3) (Figs. 2A, 5C, 5D). However, more criteria are necessary to distinguish whether i) the vein formed along the thrust surface after the latter was formed, ii) the thrust nucleated along the pre-existing vein because it represented a rock discontinuity, or, iii) both the Gréixer vein and the thrust development were coeval.

At microscope scales (Figs. 5G-K), quartz shows heterometric blocky grains (5 – 500 μm), or more often randomly oriented elongated grains with a variable (4 – 20) length to width ratio. Dynamic recrystallization mechanisms of bulging and sub-grain rotation, indicative of low to intermediate (\sim 250 – 500 $^\circ\text{C}$) deformation temperatures (e.g., Stipp et al., 2002), can be found at the quartz grain boundaries (Fig. 5G). Eventually, bulges evolved to form small (2 – 10 μm) new grains. A variable number of submicron fluid inclusions with no preferred orientation are observed in the quartz mass (Fig. 5H) conferring a milky visual appearance. Otherwise, zones with a minimum quantity of these inclusions appear as sharper areas where several chlorite crystals (Fig. 5H) and 10 – 40 μm -sized, mostly liquid-rich biphasic fluid inclusions are present. Recrystallization processes appear to be localized in these sharper areas, which also exhibit chlorite-bearing stylolites, pointing to the occurrence of dissolution-precipitation processes (Fig. 5H).

Two types of secondary anastomosing veinlets can be distinguished crosscutting the main quartz mass. The first, visible only under Plain Polarized Light (PPL), is distinguished by a decrease in the number of submicron inclusions and exhibits a gradual contact with the milky quartz host (Fig. 5I). These veinlets are 0.1 – 3 mm thick and are generally continuous. In Cross Polarized Light (XPL) these veins are in optical continuity with the host quartz crystals

with no new quartz crystal nucleation (Fig. 5J). The second typology is thicker (up to 0.6 mm), formed by individualized blocky quartz crystals, being iden-

tified in both PPL and XPL by increases in sharpness and by the presence of permeating Fe oxides along its margins.

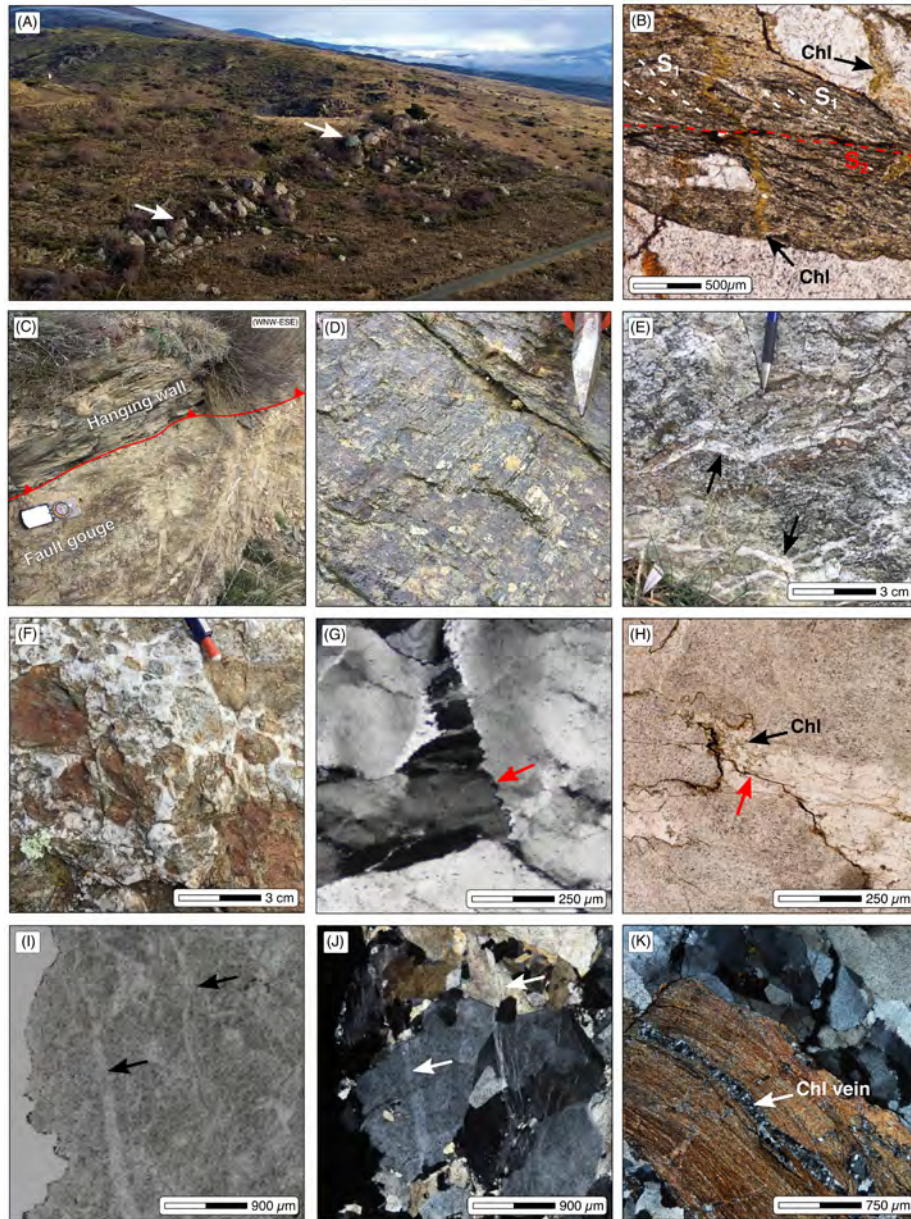


Figure 5. (A) Panoramic view of the Gréixer quartz vein (white arrows); one-lane road in the lower right corner for scale. (B) Typical fabric of the Serdinya Fm. rocks: a slaty cleavage (S_1) only visible at the microscopic scale in the pelitic layers is affected by a crenulation cleavage (S_2) that is the most recognisable surface in the study area. (C) Outcrop of the meso-scale thrust identified in the study area and (D) detail of one of the thrust surfaces showing slickensides and striae that suggest a southwards displacement of the hanging wall. (E) Centimetric- to millimetric-width veinlets crosscutting the main quartz body (black arrows). (F) Brecciated levels in the vein limits composed of heterometric host rock fragments. (G) Dynamic quartz recrystallization with bulges and small recrystallized grains (red arrow), under cross polarized light (XPL). (H) Chlorite-bearing stylolites under plane polarized light (PPL) (red arrow), with chlorite crystals growing towards the sharper areas. (I, J) Anastomosing quartz veinlets displaying optical continuity with the host quartz crystals, respectively, under PPL (black arrows) and XPL (white arrows). (K) Silicified, phyllosilicate-rich host rock fragment (Serdinya Fm.) embedded in a heterometric quartz matrix.

Phyllosilicates—mostly chlorite and muscovite as revealed by XRF diffraction—can be recognized within the host rock fragments and within the main quartz mass (Figs. 5H, 5K). Host rock-linked chlorites mostly occur as isolated euhedral-to-subhedral crystals (5 – 200 μm), or eventually with vein morphologies (Fig. 5K). Chlorites within the quartz that grow from host rock fragments occur as chrysanthemum or vermicular-shaped crystals (10 – 150 μm) in aggregates of 50 – 200 μm . In contrast, chlorites within the quartz having no relationships with host rock fragments are isolated vermicular-shaped crystals (50 μm – 1 mm). Interestingly, only few (< 10%) isolated or aggregated chlorite crystals have been identified in the milky quartz areas.

On the basis of chlorite semi-empirical thermometry, peak temperatures between 310 and 370 $^{\circ}\text{C}$ have been suggested for the host rocks coevally to the regional foliation development, whilst the formation of the main quartz bodies have registered temperatures of 140 – 180 $^{\circ}\text{C}$ (González-Esvertit et al., 2021). This difference on the formation temper-

atures was attributed to a progressive “chlorite refinement” during the quartz formation that involved changes in the texture and chemistry of the different types of chlorites.

5. Comparison with neighbouring areas

It should be noted that other Pyrenean massifs made up of low-grade Cambrian-Ordovician metasediments exhibit a similar structural arrangement to that described for the studied area: a regional crenulation cleavage, regularly oriented and moderately to steeply dipping to the north, is associated with intersection lineations and minor fold axes with a marked dispersion when developed in the Cambrian-Ordovician rocks. This disposition has been described in the La Rabassa dome (Poblet, 1991; Capellà and Bou, 1997; Margalef, 2015), the Massana anticline (Casas et al., 1998; Hartevelt, 1970; Poblet, 1991), the Orri dome (Hartevelt, 1970; Speksnijder, 1986; Poblet, 1991) and the Lys-Caillouas massif (Den Brok, 1989), among others (Fig. 1A).

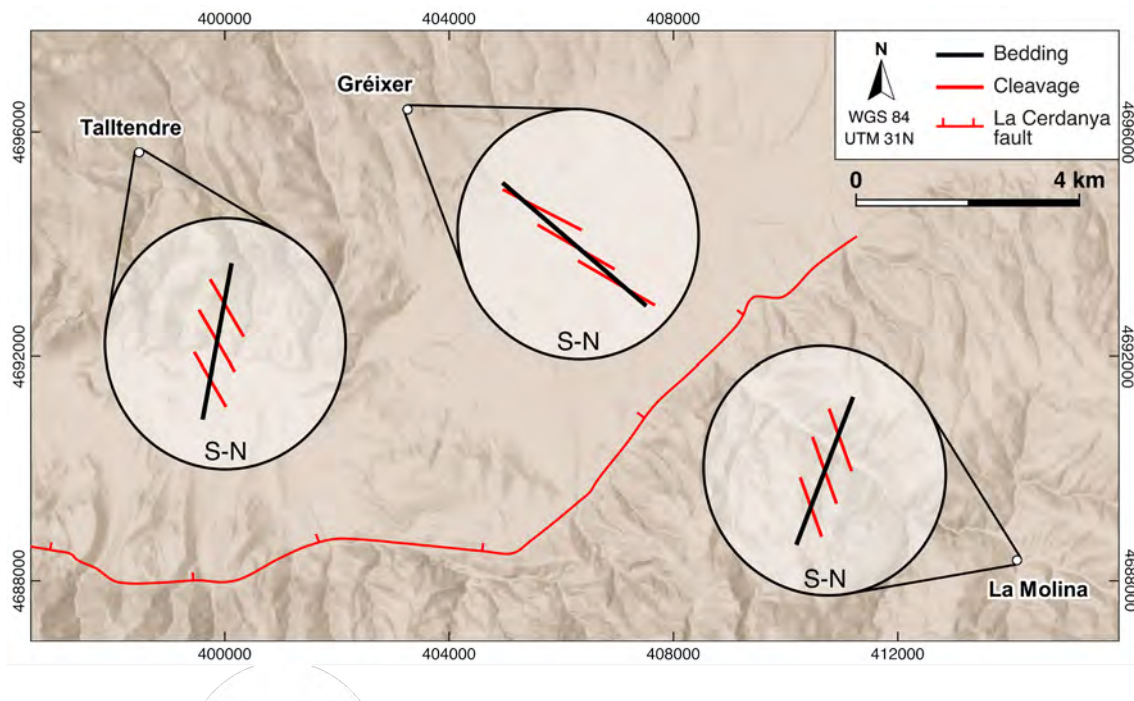


Figure 6. Structural sketch showing the bedding (S_0)-cleavage (S_2) relationships in the Gréixer, La Molina, and Talltendre sectors. Basemap: Hillshade from ©LiDARv2 data; Institut Cartogràfic i Geològic de Catalunya (CC BY 4.0).

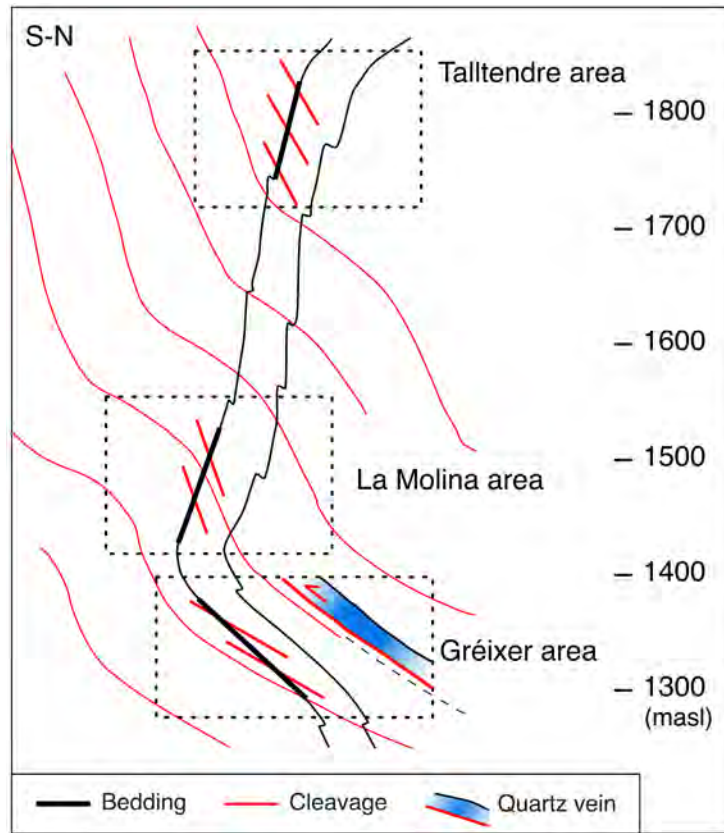


Figure 7. Structural sketch section integrating the bedding (S_0)-cleavage (S_2) relationships from the Gréixer, La Molina, and Talltendre sectors shown in figure 6. The three sectors are located in the southern limb of a first-order E-W trending south-verging D_2 antiform, which was re-folded during D_3 by south-verging folds.

When comparing in greater detail the structure described here with that of the neighbouring La Molina and Talltendre areas, some differences arise (Fig. 6). In Talltendre, bedding planes of the Upper Ordovician rocks dip strongly to the south (average value of ca. 80°) whereas the S_2 cleavage planes dip strongly to the north (average value of ca. 60°) (Puđu et al., 2019). In a similar way, bedding planes of Upper Ordovician rocks in the La Molina area dip strongly to the south (ca. 70°) and the S_2 dips ca. 70° to the north (Casas et al., 2012; González-Esvertit et al., 2020) (Fig. 6). The difference between the disposition of the S_0 and S_2 in both areas could be attributed to a hanging wall tilting of the La Cerdanya normal fault. Considering an average south-dipping value of $8 - 10^\circ$ for the Neogene beds of the La Cerdanya Basin (Cirés et al., 1994), a tilt of 10° linked to the movement of the fault may affect the Talltendre and Gréixer

areas (Figs. 2C, 6). However, this tilt is not enough to explain the different attitude of the S_0 and S_2 in Gréixer compared with that of the La Molina and Talltendre areas. The effect of a post- D_2 folding episode, affecting both the S_0 and S_2 planes, should thus be invoked (Fig. 7). Although no mesostructures related to this D_3 folding episode have been identified in the study area, in the La Molina sector Casas et al. (2012) describe D_3 open south-verging folds with axial surfaces dipping moderately to the north or northeast. D_3 folds developed across different scales and gave rise to a locally developed S_3 cleavage. Thus, we propose that D_3 folds affecting the southern limb of a kilometre-sized D_2 fold may explain the reverse limb geometry that is observed in the study area (Fig. 7). Following this idea, thrust planes and the Gréixer quartz vein might have been emplaced preferentially in D_3 fold limbs, where S_0 and S_2 dip gently to the north (Figs. 5B, 5C, 7).

6. Conclusions

The study area constitutes the south limb of a kilometre-sized E-W trending south-verging D_2 antiform of Variscan age related to the formation of a well-developed S_2 cleavage. This limb is deformed by open south-verging D_3 folds with axial surfaces that dip moderately to the north or northeast, which gave rise to the reverse limb geometry observed, as well as the different structural attitudes between the study area and the La Molina and Talltendre sectors. D_3 folds could be Variscan or Alpine in age. Differences between these areas were influenced, furthermore, by the $\sim 10^\circ$ hanging wall tilt of the La Cerdanya Neogene normal fault.

Previous to D_2 , a D_1 deformational episode of probably pre-Upper Ordovician (Mid-Ordovician?) age may be inferred at microscopic scale and from the disposition of the main phase (D_2) mesostructures and bedding surfaces in the Cambrian-Ordovician rocks. The hectometric-sized Gréixer quartz vein, probably Alpine in age, is emplaced together with other quartz bodies located northwards in the gently north dipping D_3 fold limbs, following a south-directed thrust. The mechanisms of quartz vein emplacement, together with the relationships between quartz veins and thrust development, deserve future attention.

Acknowledgements

This paper summarizes the main results of the MSc and BSc theses of E.G.E. and J.M.V., respectively. The authors are grateful for the use of MOVE[®] (Petroleum Experts) and OpenStereo[®] 0.9 (C. H. Grohmann and G. A. Campanha, University of Sao Paulo, Brazil) software packages. Useful and detailed revisions made by Elena Druguet and one anonymous reviewer have improved a first version of the manuscript. Josep Poblet and Joaquín García-Sanseguendo are acknowledged for handling this special issue on the geology of the Pyrenean Axial Zone. This paper is a contribution to the 2017SGR-1733 and 2021SGR-00349 Consolidated Research

Groups (Generalitat de Catalunya), and to projects CGL2017-87631-P and PID2021-122467NB-C22 funded by Ministerio de Ciencia, Innovación y Universidades/Agencia Estatal de Investigación/Fondo Europeo de Desarrollo Regional, Unión Europea. The PhD grant of EGE is funded by the Generalitat de Catalunya and the European Social Fund (2021 FI_B 00165). The English text was corrected by Grant George Buffett of Terranova Scientific (www.terranova.barcelona).

References

- AYORA, C. and CASAS, J. M. (1983): Estudi microtermomètric dels filons de quars de les Esquerdes de Rojà, Massís de Canigó, Pirineu Oriental. *Acta Geologica Hispanica*, 18(1): 35–46.
- AYORA, C., CARRERAS, J., CASAS, J. M. and LIESA, M. (1984): Informe quarsos. Internal report of the University of Barcelona (available under request). Barcelona, Universitat de Barcelona.
- CAPELLÀ, I. and BOU, O. (1997): La estructura del domo de la Rabassa y del sector oriental del sinclinal de Llavorsí (Pirineo Central). *Estudios Geológicos*, 53(3-4): 121–133. <https://doi.org/10.3989/egol.97533-4237>
- CASAS, J. M. (2010): Ordovician deformations in the Pyrenees: New insights into the significance of pre-Variscan ('sardic') tectonics. *Geological Magazine*, 147(5): 674–689. <https://doi.org/10.1017/S0016756809990756>
- CASAS, J. M. and FERNÁNDEZ, O. (2007): On the Upper Ordovician unconformity in the Pyrenees: New evidence from the La Cerdanya area. *Geologica Acta*, 5(2), 193–198.
- CASAS, J. M. and PALACIOS, T. (2012): First biostratigraphical constraints on the pre-Upper Ordovician sequences of the Pyrenees based on organic-walled microfossils. *Comptes Rendus Geoscience*, 344(1): 50–56. <https://doi.org/10.1016/j.crte.2011.12.003>

- CASAS, J. M., PARÉS, J. M. and MEGÍAS, L. (1998): La fábrica magnética de los materiales cambroordovícicos del Anticlinal de la Massana (Andorra, Pirineo Central). *Revista de La Sociedad Geológica de España*, 11: 317–329.
- CASAS, J. M., QUERALT, P., MENCOS, J. and GRATACÓS, O. (2012): Distribution of linear mesostructures in oblique folded surfaces: Unravelling superposed Ordovician and Variscan folds in the Pyrenees. *Journal of Structural Geology*, 44: 141–150. <https://doi.org/10.1016/j.jsg.2012.08.013>
- CAVET, P. (1957): Le Paléozoïque de la zone axiale des Pyrénées orientales françaises entre le Roussillon et l'Andorre. *Bulletin Service Carte Géologique France*, 55: 303–309.
- CIRÉS, J., DOMINGO, D., SIRVENT, J. C., SANTANACH, P., ROCA, E. and ESCUER, J. (1994): Mapa Geológico de España a escala 1:50.000, Hoja 217-Puigcerdà. *Instituto Geológico y Minero de España (IGME)*.
- CLARIANA, P. AND GARCÍA-SANSEGUNDO, J. (2009): Variscan structure in the eastern part of the Pallaresa massif, Axial Zone of the Pyrenees (NW Andorra). Tectonic implications. *Bulletin de La Société Géologique de France*, 180(6): 501–511. <https://doi.org/10.2113/gssgfbull.180.6.501>
- COCCO, F. and FUNEDDA, A. (2019): The Sardinian Phase: Field evidence of Ordovician tectonics in SE Sardinia, Italy. *Geological Magazine*, 156(1): 25–38. <https://doi.org/10.1017/S0016756817000723>
- DEN BROK, D. W. I. (1989): Evidence for pre-Variscan deformation in the Lys Caillaouas area, Central Pyrenees, France. *Geologie en Mijnbouw*, 68: 377–380.
- GARCÍA-SANSEGUNDO, J. and ALONSO, J. (1989): Stratigraphy and structure of the southeastern Garona Dome. *Geodinamica Acta*, 3(2): 127–134. <https://doi.org/10.1080/09853111.1989.11105180>
- GARCÍA-SANSEGUNDO, J., GAVALDÁ, J. and LUIS ALONSO, J. (2004): Preuves de la discordance de l'Ordovicien supérieur dans la zone axiale des Pyrénées: Exemple du dôme de la Garonne (Espagne, France). *Comptes Rendus Geoscience*, 336(11): 1035–1040. <https://doi.org/10.1016/j.crte.2004.03.009>
- GIL-PEÑA, I., BARNOLAS, A., VILLAS, E. and SANZ-LÓPEZ, J. (2004): *El Ordovícico Superior de la Zona Axial*. In: J. A. Vera (ed.): *Geología de España*, Sociedad Geológica de España and Instituto Geológico y Minero de España (SGE-IGME), Madrid, 247.
- GONZÁLEZ-ESVERTIT, E., CANALS, À., CASAS, J. M. and NIETO, F. (2020): Insights into the structural evolution of the pre-Variscan rocks of the Eastern Pyrenees from La Molina quartz veins; constraints on chlorite and fluid inclusion thermometry. *Geologica Acta*, 18: 1–XXIV. <https://doi.org/10.1344/GeologicaActa2020.18.18>
- GONZÁLEZ-ESVERTIT, E., CANALS, À., CASAS, J. M. and NIETO, F. (2021): Chlorite chemical adjustment in the Gréixer vein: Effects on thermometry. *Macla*, 25: 32–33.
- GONZÁLEZ-ESVERTIT, E., CANALS, À., BONS, P. D., MURTA, H., CASAS, J. M., and GOMEZ-RIVAS, E. (2022a). Geology of giant quartz veins and their host rocks from the Eastern Pyrenees (Southwest Europe). *Journal of Maps*, 1-13. <https://doi.org/10.1080/17445647.2022.2133642>
- GONZÁLEZ-ESVERTIT, E., CANALS, A., BONS, P. D., CASAS, J. M., and GOMEZ-RIVAS, E. (2022b). Compiling regional structures in geological databases: the Giant Quartz Veins of the Pyrenees as a case study. *Journal of Structural Geology*, 163, 104705. <https://doi.org/10.1016/j.jsg.2022.104705>
- HARTEVELT, J. A. A. (1970): Geology of the upper Segre and Valira valleys, central Pyrenees, Andorra/Spain. *Leidse Geologische Mededelingen*, 45: 167–236.
- KRIEGSMAN, L. M., AERDEN, D. G. A. M., BAKKER, R. J., DEN BROK, D. W. I. and SCHUTJENS, P. M. T. M. (1989): Variscan tectonometamorphic evolution

- of the eastern Lys-Caillaouas massif, Central Pyrenees-evidence for late orogenic extension prior to peak metamorphism. *Geologie en Mijnbouw*, 68: 323–333.
- LAUMONIER, B. (1988): Les groupes de Canaveilles et de Jujols (“Paléozoïque inférieur”) des Pyrénées orientales – arguments en faveur de l’âge essentiellement Cambrien de ces séries. *Hercynica*, 4: 25–38.
- MARGALEF, A. (2015): Estudi estructural i estratigràfic del sud d’Andorra. *PhD Thesis, Universitat de Barcelona*, 172 p.
- MARGALEF, A. and CASAS, J. M. (2016): Corte geológico compensado del sur de Andorra: Aportaciones a la estructura varisca del Pirineo central. *Geo-Temas*, 16: 61–63.
- MARGALEF, A., CASTIÑEIRAS, P., CASAS, J. M., NAVIDAD, M., LIESA, M., LINNEMANN, U., HOFMANN, M. and GÄRTNER, A. (2016): Detrital zircons from the Ordovician rocks of the Pyrenees: Geochronological constraints and provenance. *Tectonophysics*, 681: 124–134. <https://doi.org/10.1016/j.tecto.2016.03.015>
- MCCLELLAND, E. A. and MCCAIG, A. M. (1988): Palaeomagnetic estimates of total rotation in basement thrust sheets, Axial Zone, Southern Pyrenees. *Cuadernos de Geología Ibérica*, 12: 181–193.
- MUÑOZ, J. A. (1992): Evolution of a continental collision belt: ECORS-Pyrenees crustal balanced cross-section. In: K. R. McClay (ed.): *Thrust Tectonics*, Springer, Netherlands, 235–246. https://doi.org/10.1007/978-94-011-3066-0_21
- NAVIDAD, M., CASTIÑEIRAS, P., CASAS, J. M., LIESA, M., BELOUSOVA, E., PROENZA, J. and AIGLSPERGER, T. (2018): Ordovician magmatism in the Eastern Pyrenees: Implications for the geodynamic evolution of northern Gondwana. *Lithos*, 314–315: 479–496. <https://doi.org/10.1016/j.lithos.2018.06.019>
- PADEL, M., ÁLVARO, J. J., CASAS, J. M., CLAUSEN, S., POUJOL, M. and SÁNCHEZ-GARCÍA, T. (2018): Cadomian volcanosedimentary complexes across the Ediacaran–Cambrian transition of the Eastern Pyrenees, southwestern Europe. *International Journal of Earth Sciences*, 107(5): 1579–1601. <https://doi.org/10.1007/s00531-017-1559-5>
- PADEL, M., CLAUSEN, S., ÁLVARO, J. J. and CASAS, J. M. (2018): Review of the Ediacaran-Lower Ordovician (pre-Sardic) stratigraphic framework of the Eastern Pyrenees, southwestern Europe. *Geologica Acta*, 16: 339–365.
- POBLET, J. (1991): Estructura herciniana i alpina del vessant sud de la zona axial del Pirineu central. *PhD Thesis. Barcelona, Universitat de Barcelona*, 604 p.
- POUS, J., JULIA, R. and SOLE-SUGRANES, L. (1986): Cerdanya basin geometry and its implication on the Neocene evolution of the Eastern Pyrenees. *Tectonophysics*, 129: 355–365.
- PUDDU, C., ÁLVARO, J. J., CARRERA, N. and CASAS, J. M. (2019): Deciphering the Sardic (Ordovician) and Variscan deformations in the Eastern Pyrenees, SW Europe. *Journal of the Geological Society*, 176(6): 1191–1206. <https://doi.org/10.1144/jgs2019-057>
- ROEST, W. R. and SRIVASTAVA, S. P. (1991): Kinematics of the plate boundaries between Eurasia, Iberia, and Africa in the North Atlantic from the Late Cretaceous to the present. *Geology*, 19(6): 613–616. [https://doi.org/10.1130/0091-7613\(1991\)019<0613:KOTPB>2.3.CO;2](https://doi.org/10.1130/0091-7613(1991)019<0613:KOTPB>2.3.CO;2)
- ROSENBAUM, G., LISTER, G. S. and DUBOZ, C. (2002): Reconstruction of the tectonic evolution of the western Mediterranean since the Oligocene. *Journal of the Virtual Explorer*, 8: 107–130. <https://doi.org/10.3809/jvirtex.2002.00053>
- SANTANACH, P. (1972a): Estudio tectónico del Paleozoico inferior del Pirineo entre la Cerdeña y el río Ter. *Acta Geologica Hispanica*, 7: 44–49.
- SANTANACH, P. (1972b): Sobre una discordancia en el Paleozoico inferior de los Pirineos orientales. *Acta Geologica Hispanica*, 7: 129–132.

SPEKSNIJDER, A. (1986): Geological analysis of Paleozoic large-scale faulting in the south-central Pyrenees. *Geologica Ultraiectina*, 43: 1–211.

STIPP, M., STÜNITZ, H., HEILBRONNER, R. and SCHMID, S. M. (2002): Dynamic recrystallization of quartz: Correlation between natural and experimental conditions. *Geological Society, London, Special Publications*, 200(1): 171–190. <https://doi.org/10.1144/GSL.SP.2001.200.01.11>